

Article

Growth, Morphological Alterations, and Enhanced Photosynthetic Performance Promote Tolerance of *Distylium chinense* to Alternate Drought–Flooding Stresses

Lei Yue ^{1,†} , Chengrui Yu ^{1,†}, Andlia Abdoussalami ¹, Xiaoling Li ^{1,*}, Kun Lv ¹, Guiyun Huang ², Meixiang Hu ² and Zhengjian Yang ³

¹ Hubei International Scientific and Technological Center of Ecological Conservation and Management in the Three Gorges Area, Engineering Research Center of Eco-Environment in Three Gorges Reservoir Region, Ministry of Education, College of Biological and Pharmaceutical Sciences, China Three Gorges University, Yichang 443002, China; yuelei2024@foxmail.com (L.Y.)

² Hubei Key Laboratory of Rare Resource Plants in Three Gorges Reservoir Area, China Three Gorges Corporation, Yichang 443000, China

³ College of Hydraulic and Environmental Engineering, China Three Gorges University, Yichang 443002, China

* Correspondence: xiaolingli@ctgu.edu.cn

† These authors contributed equally to this work.

Abstract: Disentangling the underlying processes of plant adaptations to multiple abiotic stressors is crucial regarding promissory species for the restoration of riparian ecosystems prone to suffering extreme flood and drought events in the context of global climate change and human activities. *Distylium chinense* is a dominant evergreen shrub, distributed in the riparian areas of the Yangtze River in China. Here, one field study and five controlled experiments (Control, CK; single drought, D; single flooding, FF; from drought to recovery to full flooding, D-R-FF; from full flooding to recovery to drought, FF-R-D) were conducted. More hypertrophied lenticels, adventitious roots, and the increased stem-base hypertrophy of *D. chinense* were observed under the D-R-FF condition compared with FF and FF-R-D. Interestingly, the increase of the net photosynthetic rate (Pn) coincidentally occurred with the increase of heme degradation by heme oxygenase ($r = 0.608$, $p = 0.003$). Pn of *D. chinense* in D-R-FF was about twice as much as that in FF-R-D. The enhanced photosynthetic performance was functionally coupled with the adequate water supply to promote the tolerance of *D. chinense* to alternate drought–flooding condition compared with no any flooding condition. The accumulation of soluble sugar was highest under D, followed by FF-R-D, FF and D-R-FF, which showed that soluble sugar accumulation over the drought period could trigger the recovery growth of flooded plants in later flooding. These data provided the first insights into the tolerance mechanisms by a suite of morphological alterations and physiological adaptations, especially in the enhanced photosynthetic performance of *D. chinense* under alternating drought and flooding stresses. So, *D. chinense* could be considered as a prominent shrub species in the restoration practices of wetlands, riparian areas, and other flood-prone forests.

Keywords: *Distylium chinense*; alternate drought and flooding; single drought or flooding; morphological alterations; photosynthetic responses



Citation: Yue, L.; Yu, C.; Abdoussalami, A.; Li, X.; Lv, K.; Huang, G.; Hu, M.; Yang, Z. Growth, Morphological Alterations, and Enhanced Photosynthetic Performance Promote Tolerance of *Distylium chinense* to Alternate Drought–Flooding Stresses. *Forests* **2024**, *15*, 125. <https://doi.org/10.3390/f15010125>

Academic Editor: Heinz Rennenberg

Received: 28 November 2023

Revised: 21 December 2023

Accepted: 4 January 2024

Published: 8 January 2024



Copyright: © 2024 by the authors. Licensee MDPI, Basel, Switzerland. This article is an open access article distributed under the terms and conditions of the Creative Commons Attribution (CC BY) license (<https://creativecommons.org/licenses/by/4.0/>).

1. Introduction

Irrespective of the international consensus about the importance of wetlands and riparian areas for ecosystem health and the maintenance of biodiversity, wetlands and riparian areas are being destroyed faster than any other terrestrial ecosystem in the context of global climate change and human activities [1]. About half of this area has been lost, converted, or degraded in the last century. Among the main factors related to wetland degradation are the clearing of vegetation, agriculture, ranching, and industrial usage, as

well as environmental problems caused by global climate change and hydropower dam construction [1–4]. Every year, the flood–drought–flood cycle repeats itself. As a result, the riparian ecosystem is facing unprecedented alternating floods and drought risks, which may exacerbate the adverse impacts caused by droughts or floods [5,6]. Hydrological dynamics (e.g., the frequency and duration of flooding or droughts) have significant effects on riparian vegetation. Particularly, the repeating drought and flooding stresses could extirpate the native riparian plants and alter the vegetation patterns [7–9]. Consequently, the re-vegetation of these natural ecosystems experiencing alternate drought and flooding stresses is an important issue to be addressed, and the identification of species able to help in that process becomes essential. Therefore, it is crucial to understand the distinct morphological, physiological, and ecological adaptations of native shrubs not only under a single drought or flooding period but also under alternate drought and flooding stresses for restoration efforts in degraded riparian ecosystems.

Plants experiencing different hydrological conditions could respond to various regime variations through morphological, physiological, and ecological adaptations that help them cope with such variations [10–13]. Plant populations from different positions are subjected to various regimes of flooding and drought, both of which may also occur in the same growing season. Flooding and submergence pose considerable challenges for plant growth and survival [14]. During flooding, the transmission of gases such as O₂, CO₂, and ethylene into the water is relatively slow. Cellular O₂ levels are reduced, inhibiting aerobic respiration [15,16]. But, within limits imposed by flooding depth, duration, timing, and intensity, they can, in some tolerant species, be overcome by appropriate combinations of growth, morphological, and eco-physiological attributes or adaptations [15,17–19]. The flood-tolerant species respond to flooding by morphological changes such as the development of intercellular spaces in lenticels, an increase in stem-base growth, the formation of adventitious roots, and aerenchyma development [15,20,21]. The photosynthetic rate and stomatal conductance of flooded seedlings also were lowered with an increase in flooding depth. The recovery of the reduced photosynthetic rate and stomatal conductance occurred simultaneously with the advancement of adventitious root formation in the flooded seedlings [20].

Flooding reduces water absorption and stomatal conductance, causing flooding-sensitive plants to wilt in a similar way to drought [22]. And water shortages are getting worse due to the increased evapotranspiration, precipitating more frequent and intense drought events and inhibiting the growth of plant shoots and roots and their photosynthesis, ultimately resulting in plant death [23]. Various plant species and populations have highly varying drought tolerances, acclimatization rates, and acute drought responses [24–26]. Under moderate and severe drought stress, the accumulation of soluble sugar is mediated by osmoprotection in plants to reduce stress damage [27]. Aside from alterations in photosynthetic responses and the accumulation of soluble sugar, drought triggers a range of different cellular interactions; for example, it changes the entire plant transcriptome and metabolome [28,29]. Therefore, the search for general adaptive syndromes evolved by plants to tolerate multiple co-occurring or subsequent abiotic stressors is of uttermost importance to foresee species responses to current and future climatic change.

Distylium chinense (Fr.) Diels is an evergreen and native shrub that belongs to the genus *Distylium* of Hamamelidaceae [30]. This genus is found in China, Indonesia (Java and Sumatra), Northeast India (Assam), Japan (Ryukyu Islands), Korea, and Malaysia, particularly distributed in the riparian areas and wetlands of China's Yangtze River [4,30]. Its seedling survival rate reached more than 90% at an altitude of 175 m in the Three Gorges reservoir area of China [21]. In addition, this species frequently grows as a charming ornamental shrub that is found in parks, green spaces, and around lakes, and it is cultivated as a potted flowering plant for its beautiful red inflorescences, or as a hedge and ground cover plant for landscaping [4], which showed that *D. chinense* has great ornamental value and great social and economic benefits.

However, due to the construction of hydroelectric projects like the Three Gorges Dam and other anthropogenic activities such as overharvesting and excavating, the wild populations of *D. chinense* are in steep decline [4]. And it was classified as endangered according to China's Higher Plants Red List (CHPRL). Today, the search for alternative species capable of tolerating multiple stresses such as alternate drought and flooding is one of the main objectives in protecting and conserving the ecosystem biodiversity in the face of global climate change and intensified human activities. Previous studies have mainly concentrated on the morphological and photosynthetic responses to a single flooding event [17,21]. General patterns and mechanisms describing this species' adaptations to tolerate multiple abiotic stressors such as alternate drought and flooding stresses remain poorly understood. Therefore, it is imperative to obtain knowledge on the growth, morphological, and physiological adaptive responses of *D. chinense* to the alternate hydrological conditions (D-R-FF and FF-R-D) to provide information on how to use this species for restoration and reconstruction programs of the degraded riparian ecosystem. The following three hypotheses were examined:

- (1) *D. chinense* exhibits differences in growth, morphological, and physiological activity alterations under alternate hydrological regimes (D-R-FF and FF-R-D) compared with single drought and flooding events.
- (2) The enhanced photosynthetic performance was functionally coupled with the adequate water supply to promote the tolerance of *D. chinense* to alternate drought–flooding condition. Drought in the early stage could promote the tolerance of *D. chinense* to flooding in the later stage.
- (3) More hypertrophied lenticels and adventitious root occurrence may be attributed to the enhanced heme oxygenase (HO) activities of *D. chinense* seedlings. It may be a vital adaptation to the D-R-FF hydrological regime.

2. Materials and Methods

2.1. Experimental Materials

D. chinense (Figure 1A–D) is a perennial shrub of the *Distylium* genus of the Hamamelidaceae family. Adventitious branches from deep-seated rhizomes generate dense colonies. It can reach a height of 0.8 to 1.2 m and has a large root system. Leaf blade is elliptic to oblanceolate, 2–4 cm long, 1–1.2 cm wide, both surfaces glabrous, base broadly cuneate, margin entire or with two or three teeth on each side near apex, apex subacute; lateral veins five per side, reticulate veins obscure on both surfaces; petiole is densely lepidote and 1.5–2 mm long; lateral veins five per side. It germinates seeds in the autumn and blooms in the early spring [30]. *D. chinense* of the population is a perennial shrub with adventitious branches that emerge from deep-seated rhizomes to produce dense colonies. It has a well-developed root system and is considered an ideal protective shrub species along riparian areas [30].

D. chinense seedlings (about 15 cm in height) were gathered and transported to Yichang, Hubei Province, China, in soft-walled containers to lessen root loss throughout excavation and transport. The soil–sand mixture contains 30% yellow-brown soil, 30% coarse-grained sand (1–2.2 mm), 30% fine-grained sand (0.7–1.22 mm), and 10% perlite. It also has a soil bulk density of 1.38 g cm^{−3}.

The seeds were placed into plastic containers that measured 17.5 cm wide by 15 cm high for all the seedlings. The plants were kept in well-aerated soil conditions and allowed to grow outdoors for at least 6 months with one seedling in each container before the soil-flooding treatments began. Every other day, tap water was used for irrigation. We only used seedlings with robust roots. The experiments were conducted in ecological experimental station of China Three Gorges University, Yichang city, Hubei province, China (111°18' E, 30°43' N, 133 m).



Figure 1. The photos display normal leaves (A), branches (B), flowers (C) and seeds (D) of *D. chinense*, and its growth is particularly vigorous in riparian areas.

2.2. Sampling Sites and Field Studies

We selected two 20 m × 20 m sampling sites (Site 1 and Site 2) (111°23' E, 30°53' N, 212.91 m; 111°48' E, 30°45' N, 130.15 m) that experienced alternate drought–flooding condition (DF) and no any flooding condition (NF) during the growing season, respectively. Basic environmental information on sampling sites and geographic distribution map is shown in Table 1 and Figure 2. Under DF condition, seasonal floods occurred from May to September and quickly increased from 5 cm to 100 cm. The submerging duration was no more than 30 days. Furthermore, natural precipitation and agriculture drainage are responsible for variations in water levels. Between September and April of the following year, dry soil layers can be found. In both sampling sites, *D. chinense* was the dominant species at both sampling sites (Site 1 and Site 2). Three fixed quadrats (5 m × 5 m) were randomly located within each site. We used a portable photosynthesis system (Li-6400, LI-COR, Lincoln, NE, USA) under PAR near the light-saturation region ($1200 \text{ mol m}^{-2} \text{ s}^{-1}$) with controlled

CO₂ concentration to measure net photosynthetic rate (Pn), stomatal conductance (Gs), intercellular CO₂ concentration (Ci), transpiration rate (Tr), and CO₂ concentration of the air (Ca) of the third fully expanded leaf from the shoot tip. The measurement periods from 9:00–11:00 a.m. had a controlled CO₂ concentration of 380 $\mu\text{mol CO}_2 \text{ mol}^{-1}$. Leaf temperature was 20 °C and relative humidity 60%–70% every two hours (five times within a day). All measurements of the field were repeated three times. The water-use efficiency (WUE) and stomatal-limiting value (Ls) were calculated according to the following formulas:

$$WUE = \frac{Pn}{Tr}$$

$$Ls = 1 - \frac{Ci}{Ca}$$

Table 1. Basic environmental information of sampling sites (Site 1 and Site 2). Values are means \pm SE, n = 3.

	Latitude and Longitude	Soil Water Content (%)	Air Humidity (%)	Light Intensity/ $\mu\text{mol}\cdot\text{m}^{-2}\text{ S}^{-1}$	Air Temperature (°C)
Site 1	111°23' E, 30°53' N, 212.91 m	30.37 \pm 0.73	82.00 \pm 1.73	1417.7 \pm 55.0	25.00 \pm 0.58
Site 2	111°48' E, 30°45' N, 130.15 m	21.40 \pm 0.59	55.33 \pm 1.33	1343.3 \pm 17.8	30.67 \pm 0.88

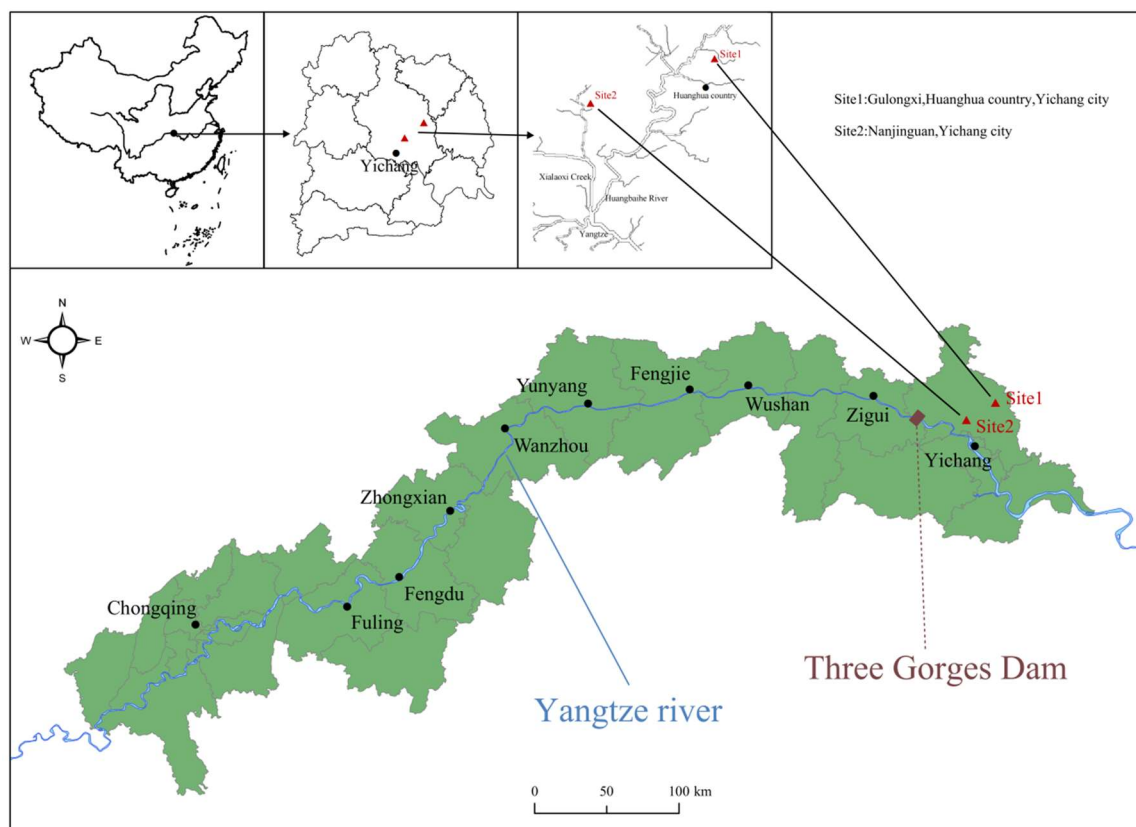


Figure 2. Sampling sites (Site 1 and Site 2) of field photosynthesis of *D. chinense*.

2.3. Experimental Design

One-year-old *D. chinense* seedlings were transplanted into plastic containers (with 3.5 kg soil, 17 cm diameter). All the seedlings were cultivated in the same environment. Outdoor studies were undertaken after a 6-month acclimatization period under regular conditions of well-watered and well-drained soil. Before starting the treatments, seedlings of *D. chinense* had a mean height of 17.5 ± 1.2 cm and a mean stem diameter of 2.82 ± 0.3 mm. Among these seedlings, a total of 146 seedlings with uniform size and development were

chosen and divided into two groups of 50 seedlings at random. One group was separated into three subgroups of 16 plants, each of which was subjected to different floods of varying depths (roots, partial, and full submergence). The other group, which was watered and well-drained, was treated as non-flooded (Drought and CK). Experiments were arranged in a randomized complete block design with five replications. In this controlled experiments, all the seedlings were submitted to five treatments: (1) 25 seedlings daily watering and unflooded as a control (Unflooded, CK); (2) 25 seedlings with drought (D) treatments (topsoil: 0–10 cm depth, continuous drought with no watering for 28 days with $8.33 \pm 3\%$ of the final soil water content; (3) 16 seedlings flooded (RF) at 1 cm above the ground level (GL) for 28 days; (4) 16 seedlings partially flooded (PF) at 12 cm above the GL for 28 days; and (5) 16 seedlings fully flooded (FF) under 1.2 m of deep water for 28 days. After 6 weeks (28 days for these single stresses and a recovery period of 2 weeks each), two different alternative treatments (ALs) for 2 weeks were established: 16 seedlings from drought to recovery to full flooding (D-R-FF) and 16 seedlings from full flooding to recovery to drought (FF-R-D). All the plants were grown under identical conditions and received regular care, such as weeding. The physio-chemical parameters of soil and tap water are shown in Table 2.

Table 2. The physio-chemical parameters of the soil and floodwater. Values are means \pm SE, $n = 5$.

	Temperature ($^{\circ}$ C)	pH	EC/mS cm^{-1}	Soil Water Content/%	Organic Matter/mg kg^{-1}	TN/mg g^{-1}	TP/mg g^{-1}
Soil	13.51 ± 0.27	6.67 ± 0.07	0.87 ± 0.12	32.37 ± 1.45	22.42 ± 0.46	2.08 ± 0.15	0.86 ± 0.07
Floodwater	14.32 ± 0.33	7.27 ± 0.08	0.46 ± 0.04	-	-	0.64 ± 0.24	0.05 ± 0.00

The position of each plant was rotated randomly every week to reduce the effect of location. At the same time, to fully simulate the low-light-intensity environment caused by the turbidity of the water in the reservoir's water-leveling zone, a layer of a neutral shade cloth was laid above the pool. All plants were not fertilized during the experiment. The species' morphological characteristics were observed during 28 days after the initial flooding/drought. The plant height, epicormic shoots, and adventitious roots growing on stems and stocks were counted. At the end of the flooding/drought, 50 seedlings were chosen at random to count the number of adventitious roots and lenticels on stems, as well as measure plant height and stem diameter with a measuring tape and a digital vernier caliper, respectively. Then, the seedlings were harvested, separated into leaves, stems, epicormic shoots, roots, and adventitious roots, and their dry weights were determined separately after 48 h of drying at 80 degrees. After the recovery period, two different alternative treatments (ALs) were established for D-R-FF and FF-R-D, respectively. Morphological characteristics, photosynthetic rate, heme oxygenase activity, chlorophyll content, soluble sugar content, and soil concentrations of total nitrogen (TN) and total phosphorus (TP) were shown in the following experiments. Figure 3 presents the experimental design drawing.

2.4. Measurement of Growth Parameters

Seedling height was measured on the main stem, from the base to the apex with a ruler. Stem diameter was measured using a digital caliper positioned at the base of the main stem. The growth in height and diameter was calculated as the difference between both dates of measurements. During the treatments, per plant, the adventitious roots and stem lenticels that were visible above the soil's surface were counted. Before and after the drought or flooding incidents, all the seedling shoots were counted. Plants that had fresh leaves at the conclusion of the recovery time were considered to be alive and to have begun to grow once again. Otherwise, they were regarded as having perished.

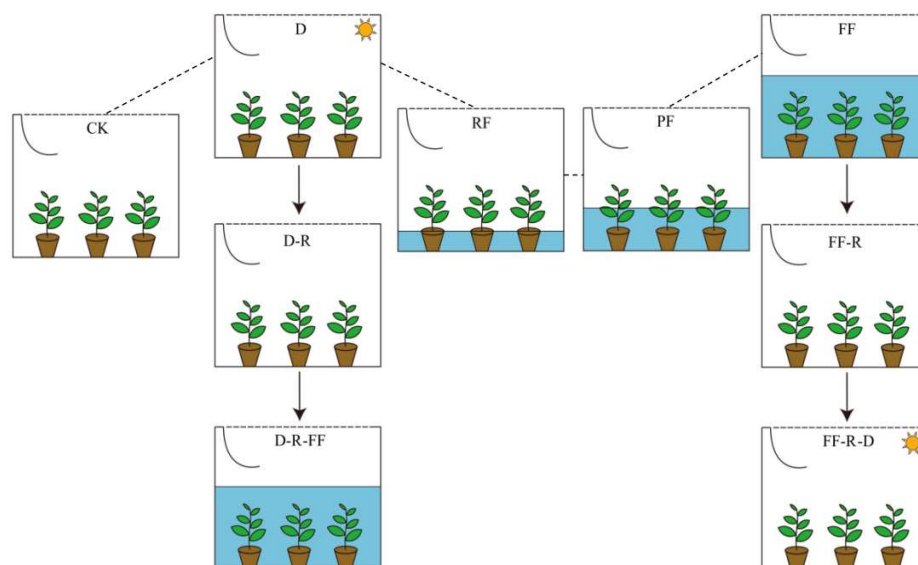


Figure 3. Experimental design drawing. The treatments of D, RF, FF, and PF were the single stress each for 28 days: CK (control), D (drought), RF (root flooded), FF (fully flooded), PF (partially flooded); D-R (drought recovery) and FF-R (flooding recovery) were 2 weeks recovery period; D-R-FF and FF-R-D were alternate drought and flooding stresses for 2 weeks respectively.

2.5. Measurement of Chlorophyll Content

Chlorophyll content (Chl) was measured on Day 1 before starting, as well as on Day 28 after flooding/drought and on recovery and alternate days. Measurements were applied on mature leaves (from the second to fifth node from shoot apices on the stem) in each of the five replicate plants. The samples were then identified using a UV-1200 ultraviolet-visible spectrophotometer. The mean value was obtained to calculate the photosynthetic pigment content per unit of fresh weight of leaf [31].

2.6. Measurement of Photosynthesis Parameters

With a portable photosynthesis system (Li-6400), photosynthetic parameters were measured on each period. The well-expanded, matured, and developed leaves were chosen at the second to fifth node from shoot apices from 9:00 to 11:00 a.m. to minimize noon photosynthetic depression. To ensure the leaves acclimate to the ambient conditions inside the leaf cuvette, the photosynthetic apparatus worked for 20 min before the measurements. The following variables must be present: leaf temperature (Tl), atmosphere temperature (Ta), Ca, Gs, Tr, Ci, Pn, and other photosynthetic parameters. It was determined what their average values were based on the CO₂ concentration in the air for Ca and Ci, as well as *Ls* for photosynthesis [32–35]. All measurements were repeated five times.

2.7. Extraction and Determination of Soluble Sugar

Soluble sugar content was measured in leaves at the beginning and end of each duration treatment, as well as two-week alternate intervals. Fifty milligrams of the dried leaf samples were weighed, 6 mg of 80% ethanol were added, it was extracted at 80 °C for 30 min, centrifuged at 3000 rpm for 5 min, and then transferred to a water bath at a constant temperature of 85 °C. In order to evaporate the ethanol until it measures 2–3 mL, it was transferred into a 50 mL volumetric flask, the volume was diluted with distilled water, and 1 mL of the liquid supernatant was drawn, while 5 mL of anthrone reagent were added to mix and boiled within 10 min. The procedures above yielded soluble sugar. Then, after cooling down, 3 mL of pure water were poured into the soluble sugar sediments and placed into the pot water (100 °C) for 15 min. After boiling, 2 mL of perchloric acid (9.2 mol/L) were added for each of them. It was centrifuged three times, and then 50 mL of pure water were added. A 1 mL solution was then mixed with 5 mL of anthrone solution

and then placed in boiling water for 10 min. The content of soluble sugar and starch was determined by determining the absorbance at 625 nm with a spectrophotometer as the previous calculation data.

2.8. Data Processing

Standard error (SE) and arithmetic means were used to calculate the values of plant morphological characteristics. All statistical analyses were undertaken in RStudio4.2.2. To identify the various periods in chlorophyll concentration, soluble sugar content, the concentration of heme oxygenase and photosynthetic characteristics of leaves, and soil environmental factors, one-way analysis of variance (ANOVA) was performed.

3. Results

3.1. Field Studies: Photosynthetic Responses

DF and NF of photosynthetic parameters are shown in Figure 4A–E. Pn, Gs, Ci, Tr, and WUE in DF were significantly higher than those in NF, respectively ($p < 0.05$). Pn in DF was 52.8% higher than that in NF, reaching $14.067 \mu\text{mol}\cdot\text{m}^{-2}\cdot\text{s}^{-1}$ on average; Gs in DF was 27.59% higher than that in NF; Tr in DF was 14.14% higher than that in NF; WUE in DF was 30.74% higher than that in NF, reaching $6.258 \mu\text{mol}\cdot\text{mol}^{-1}$ on average. Ci in NF was 25.5% lower than that in DF. As shown in Figure 5, under the DF condition, Pn was positively associated with Gs ($r = 1, p < 0.01$), Tr ($r = 0.88, p < 0.001$), and WUE ($r = 0.89, p < 0.001$). However, there existed a negative correlation between Pn and Ci ($r = -0.49, p < 0.01$). And the correlation between Ci and Gs in DF was negatively significant ($r = -0.48, p < 0.01$). In contrast, the correlation between Ci and Gs in NF was strongly positive ($r = 0.98, p < 0.01$). WUE was negatively associated with Gs ($r = -0.98, p < 0.01$) in NF. The correlations between Gs and Tr in DF ($r = 0.89, p < 0.01$) and NF ($r = 1, p < 0.01$) were both significantly positive, respectively.

3.2. Morphological Variations and Plant Growth under Single Drought, Flooding, and Alternate Drought and Flooding Stresses

In relation to its morphology under single-stress treatments, a slight increase (FF > D > CK) in stem diameter was accompanied by the development of hypertrophied lenticels (D > FF > CK) at the stem base (Table 3). The primary roots of all flooded seedlings became black, some of which even decayed to death with prolonged flooding. And adventitious roots and stem lenticels occurred significantly in the FF seedlings with prolonged flooding. However, all the flooded seedlings' stem lenticels vanished shortly after soil draining (recovery). Similarly, adventitious roots and stem lenticels of drought seedlings occurred significantly compared with fully flooded seedlings (D > FF). In addition, more hypertrophied lenticels and adventitious roots occurred significantly in the D-R-FF treatment, compared with CK, FF, and FF-R-D (Table 3; Figure 6). The roots of the drowned seedlings in the D-R-FF of roots became black, and the blades of the FF-R-D shrank (Figure 6).

Table 3. ANOVA analysis of *D. chinense* different drought and flooding treatments on morphological variations and plant growth. Values are means \pm SE, $n = 5$. CK (control); D (drought); FF (fully flooded); D-R-FF (from drought to recovery to full flooding); and FF-R-D (from full flooding to recovery to drought). Various lower-case letters indicate statistically significant variations ($p < 0.05$).

Treatments	Plant-Height Increment (cm)	Stem-Diameter Increment (cm)	Number of Adventitious Roots	Number of Stem Lenticels	Number of Epicormic Shoots
CK	4.37 ± 0.21 b	0.13 ± 0.02 c	0.00 ± 0.00 c	0.00 ± 0.00 c	8.74 ± 0.56 a
D	2.05 ± 0.19 d	0.22 ± 0.04 e	8.20 ± 0.84 b	22.40 ± 1.82 a	5.80 ± 1.92 c
FF	1.47 ± 0.34 c	0.25 ± 0.07 c	5.20 ± 0.45 b	16.00 ± 2.12 a	4.60 ± 1.14 b
FF-R-D	0.86 ± 0.22 c	0.22 ± 0.04 c	4.60 ± 0.55 b	19.20 ± 1.79 a	1.20 ± 0.84 c
D-R-FF	1.89 ± 0.12 d	0.32 ± 0.07 e	13.40 ± 1.34 b	24.20 ± 1.10 a	6.40 ± 0.89 c

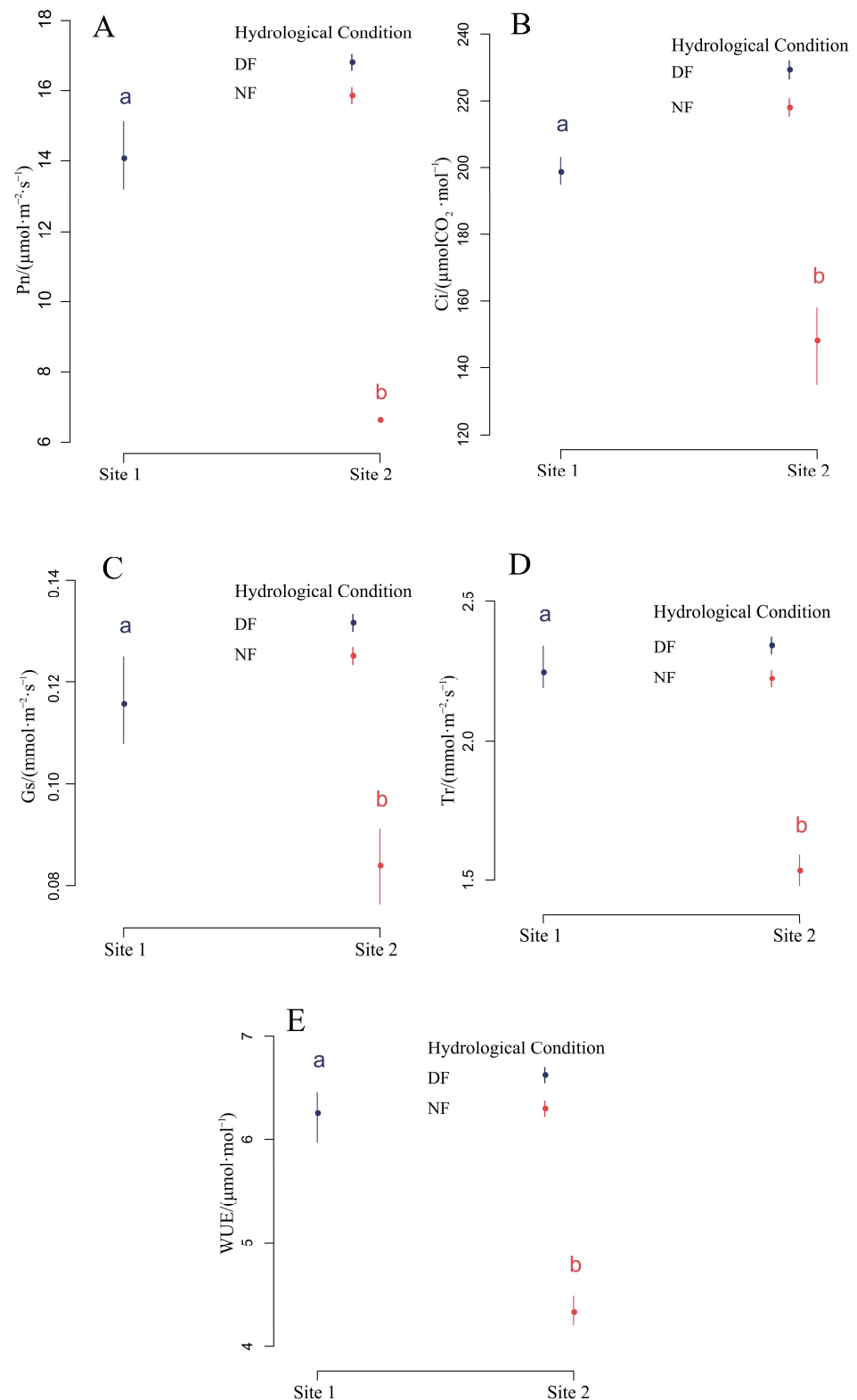


Figure 4. Effects of drought–flooding condition (DF) and no any flooding condition (NF) on photosynthetic characteristics of *D. chinense*. Values are means \pm SE, $n = 3$. Various lower-case letters indicate statistically significant variations ($p < 0.05$). Photosynthetic parameters were measured from population distribution sites in Three Gorges Reservoir area, China. The habitat of *D. chinense* on Site 1 is drought–flooding (DF) condition, Site 2 is no flooding (NF) condition. (A) Pn “net photosynthetic rate”; (B) Ci “intercellular CO_2 concentration”; (C) Gs “stomatal conductance”; (D) Tr “transpiration rate”; (E) WUE “water-use efficiency”.

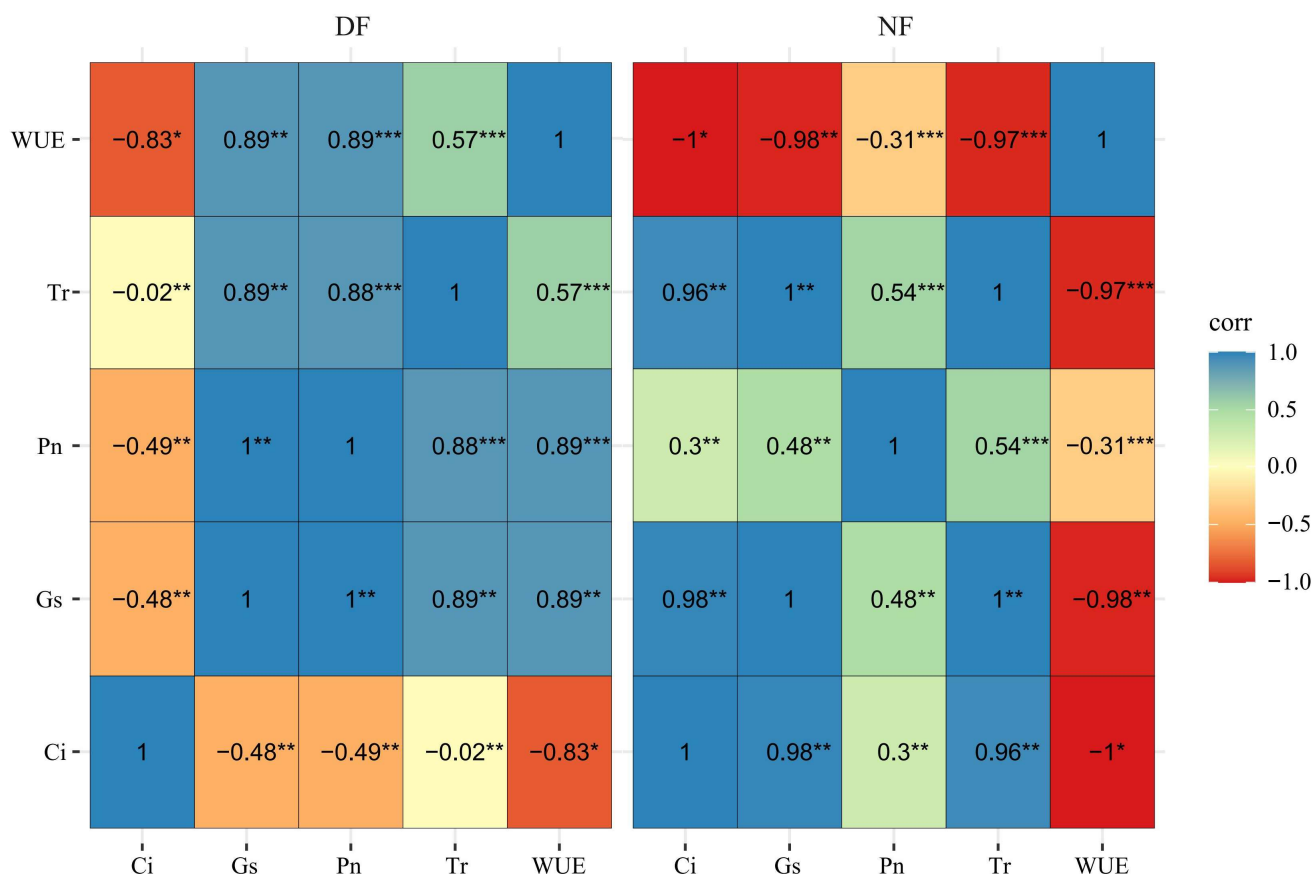


Figure 5. Correlation of drought–flooding condition (DF) and no any flooding condition (NF) on photosynthetic parameters of *D. chinense*. Pn “net photosynthetic rate”; Gs “stomatal conductance”; Ci “intercellular CO₂ concentration”; Tr “transpiration rate”; WUE “water-use efficiency” (“****” $p < 0.001$, “***” $p < 0.01$, “**” $p < 0.05$).

Regarding *D. chinense* seedling growth, a significant difference was observed at 28 days after single stresses. D and FF had an increase in plant height and epicormic shoots, respectively ($D > FF$). And after alternate treatments, plant height and epicormic shoots significantly increased in the D-R-FF, compared with FF and FF-R-D (Table 3). As also shown in Table 3, under alternate conditions, plant height and epicormic shoots in the FF-R-D almost stopped growing compared with the D-R-FF.

3.3. Effects of Single and Alternate Drought and Flooding Stresses on Chlorophyll Content

Our findings revealed that the content of Chl a, Chl b, and Chl (a + b) in the D-R-FF was significantly higher than FF and alternating FF-R-D (Figure 7). And multiple abiotic regimes had substantial impacts on leaf Chl a (Figure 7A), Chl b (Figure 7B), Chl (a + b) (Figure 7C), and their ratio (Chl a/Chl b) (Figure 7D). The content of Chl a in the FF-R was 15.14% less than that in the D-R (Figure 7A). And the content of Chl b in the FF-R was 32.07% less than that in the D-R (Figure 7B). The content of Chl a in the FF-R-D was 8.45% less than that in the D-R-FF (Figure 7A). And the content of Chl b in the FF-R-D was 20.15% less than that in the D-R-FF (Figure 7B). It was obvious that the content of Chl a, Chl b, and Chl (a + b) in the D-R-FF was higher than that in the FF-R-D (Figure 7A–C), while Chl a/Chl b content was 13.56% less than that in the FF-R-D (Figure 7D).

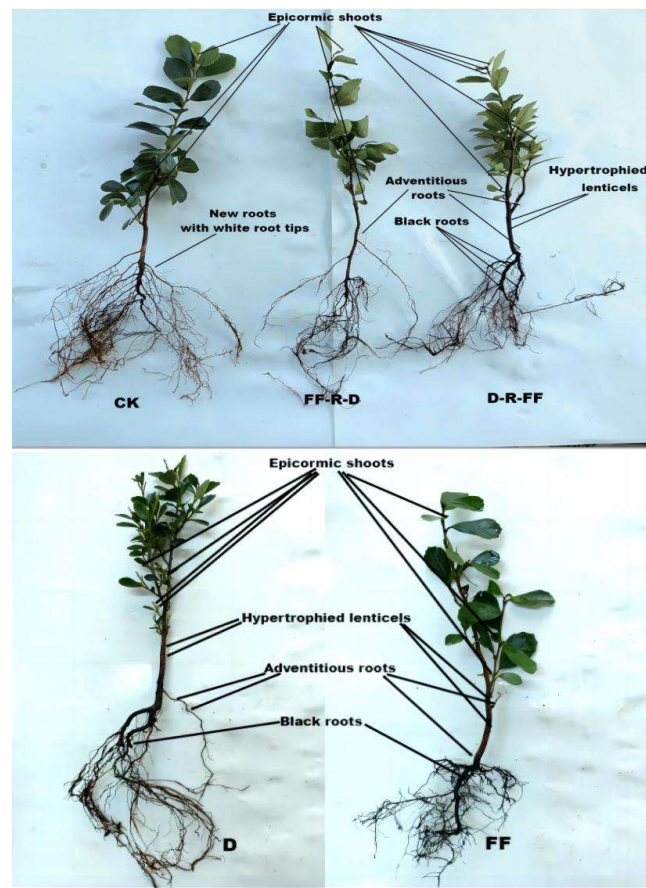


Figure 6. Morphological variations of *D. chinense* seedlings with 5 treatments: control (CK), from full flooding to recovery to drought (FF-R-D) treatment, from drought to recovery to full flooding (D-R-FF) treatment, drought (D) treatment, fullflooding (FF) treatment.

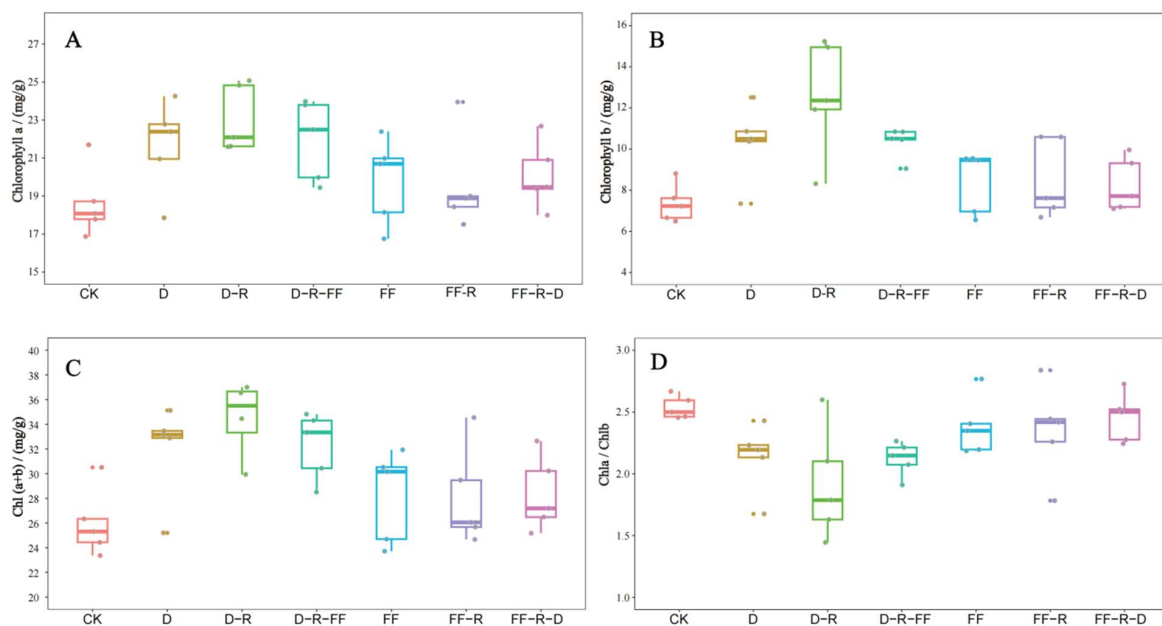


Figure 7. Distribution of *D. chinense* seedlings on changes of Chl components: Chl a (A), Chl b (B), Chl (a + b) (C), and Chl a/Chl b (D). CK (control); D (drought); FF (fully flooded); D-R (drought-recovery), and FF-R (flooding-recovery); D-R-FF and FF-R-D were alternate drought and flooding stresses. Colors indicate different Chl components and counts.

3.4. Effects of Single and Alternate Drought and Flooding Stresses on Photosynthesis

Our findings revealed that Pn in the condition of FF was higher than that in D (Figure 8). And *D. chinense* had a good recovery on photosynthetic capacity after drought or flooding (the D-R and the FF-R). However, the subsequent flooding treatment (D-R-FF) and drought treatment (FF-R-D) had a distinction on Pn between each other, and Pn of the D-R-FF was about twice as much as the FF-R-D on average value. The results showed that the photosynthetic rate of D decreased to the lowest level after the single stress, followed by the FF-R-D. However, Pn in the D-R-FF has a relatively higher photosynthetic rate than in single stresses (D and FF) and alternating FF-R-D. Therefore, it could be demonstrated that *D. chinense* had extremely great plant resilience facing alternate drought and flooding stresses, especially in the D-R-FF (Figure 8). In addition, during the subsequent 2-week recovery period, the Pn of the D-R and the FF-R showed a much faster recovery, respectively.

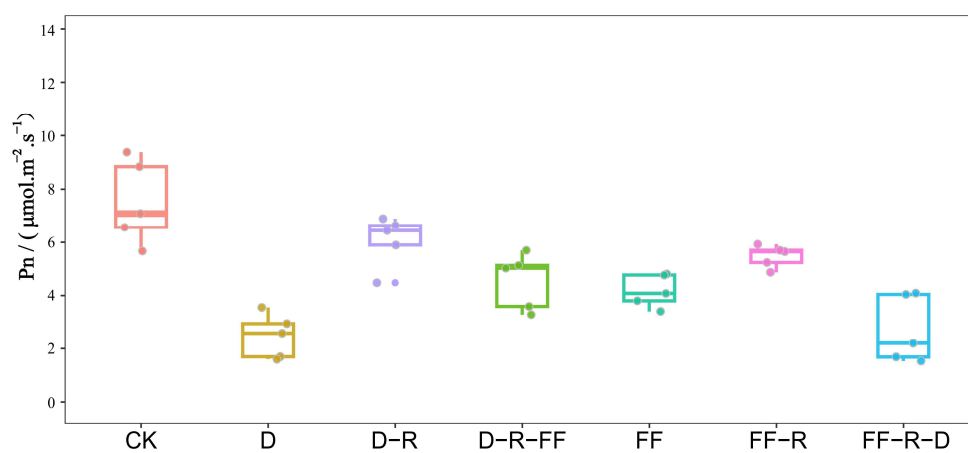


Figure 8. Seven different treatments on net photosynthetic rate (Pn) with *D. chinense* seedlings presented. CK (control); D (drought); FF (fully flooded); D-R (drought-recovery) and FF-R (flooding-recovery); D-R-FF (from drought to recovery to full flooding) and FF-R-D (from full flooding to recovery to drought). The central line in the box plots represents the median value. The lower and upper box limits correspond to the net photosynthetic rate threshold.

3.5. Correlation of Heme Oxygenase and Net Photosynthetic Rate about Different Hydrological Regimes

Linear regression analysis showed that the relationship between those hydrological regimes (D, FF-R-D, FF, D-R-FF) of Pn and HO was positively significant ($r = 0.608$, $p = 0.003$) (Figure 9). The increase in Pn was due to the increased heme degradation by HO. Pn in the D-R-FF exerted a relatively higher photosynthetic rate than in FF, followed by FF-R-D and D (D-R-FF > FF > FF-R-D > D), which was consistent with the degradation trend of each hydrological regime of heme by HO (D-R-FF > FF > FF-R-D > D).

3.6. Effects of Single and Alternate Drought and Flooding Stresses on Soluble Sugar Content

The accumulation of soluble sugar was the highest under drought stress. And after the recovery period, the soluble sugar content of *D. chinense* decreased. Our alternate stress experiment revealed that the D-R-FF (CK→D→D-R→D-R-FF) pathway (Figure 10A) was a process of continual decline in soluble sugar content (from 16.279 mg/g to 6.354 mg/g on average), maintaining the normal intracellular metabolism of seedlings (Figure 10A). Under such stress conditions, the metabolism of soluble sugar is a dynamic process that may involve simultaneous degrading and synthetic reactions. However, the FF-R-D (CK→FF→FF-R→FF-R-D) pathway (Figure 10B) did not clearly perform such a regular process. This indicated that *D. chinense* seedlings resisted drought stress by accumulating more soluble sugar, and that subsequent flooding may substantially help to alleviate alternate stress. Moreover, the soluble sugar content was the lowest in the D-R-FF (6.354 mg/g), followed

by FF (6.655 mg/g). This indicated that *D. chinense* seedlings were less sensitive to the D-R-FF hydrological condition compared with alternating FF-R-D and single FF and D.

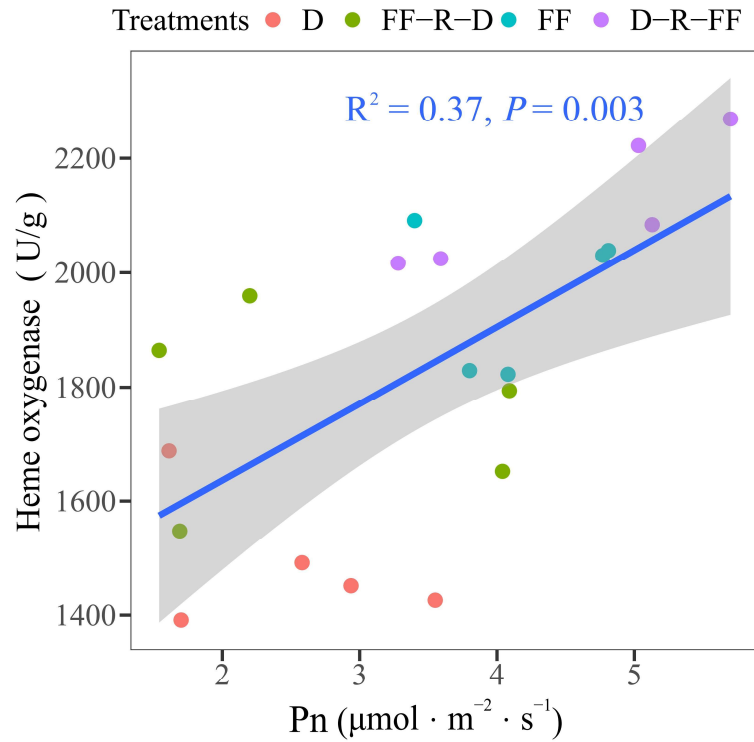


Figure 9. Linear regression analysis of heme oxygenase (HO) and net photosynthetic rate (Pn) about four hydrological regimes: D (drought), FF-R-D (from full flooding to recovery to drought), FF (fully flooded), and D-R-FF (from drought to recovery to full flooding).

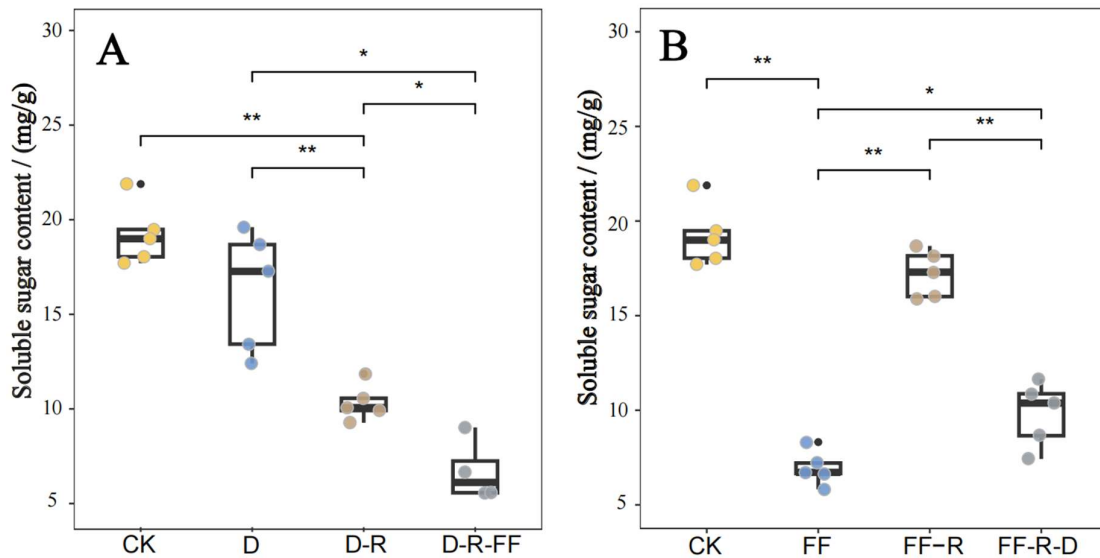


Figure 10. The soluble sugar content of *D. chinense* leaves. (A) An alternate stress pathway: from drought to recovery to full flooding. (B) Another alternate stress pathway: from full flooding to recovery to drought. CK (control), D (drought), FF (fully flooded), D-R (drought-recovery), FF-R (flooding-recovery), and two types of alternate drought and flooding stresses of D-R-FF and FF-R-D are also presented. Single stress with drought and flooding each for 28 days. The colored dots indicate different soluble sugar content. The median line in box plots represents the median value. A threshold is represented by the box’s lower and upper boundaries. Significant differences in the average soluble sugar are indicated by an asterisk (*). (Tukey’s HSD test, “***” $p < 0.01$, “**” $p < 0.05$).

3.7. Effects of Single and Alternate Drought and Flooding Stresses on Soil Nitrogen and Phosphorus Releasing

Single drought and flooding stresses, as well as alternate drought and flooding stresses, had nearly similar concentration distributions of TN but had significant influences on TP. TP in the D (1.894 mg/g) was higher than that in D-R-FF (1.298 mg/g), followed by FF (1.069 mg/g) and FF-R-D (0.802 mg/g) on average, which showed that P releasing in the soil is significantly affected by different hydrological conditions, while N releasing was not significantly affected by different hydrological conditions (Figure 11).

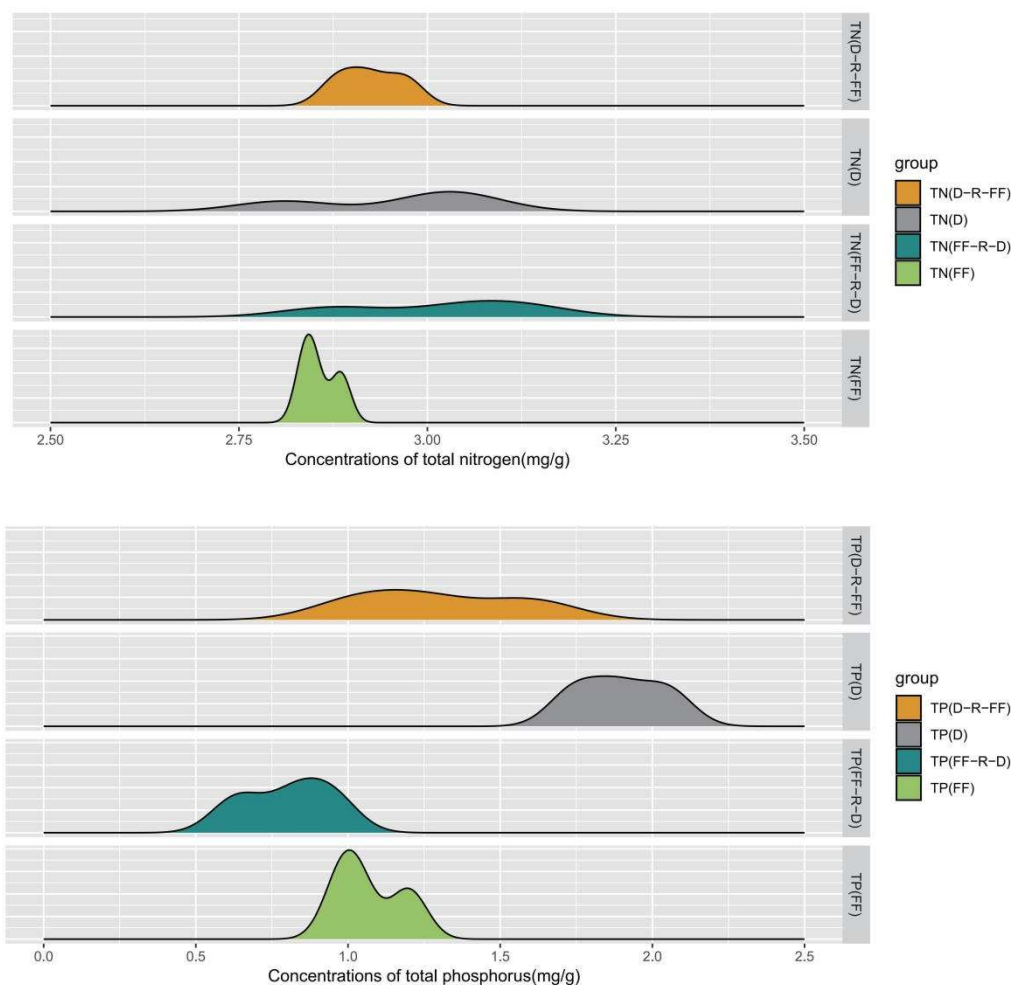


Figure 11. Soil concentrations of total nitrogen (TN) and total phosphorus (TP) in single and alternate stresses of drought and flooding (D, FF, D-R-FF, FF-R-D). The x-axis is defined as the concentration of TN and TP (mg/g).

4. Discussion

4.1. Growth, Morphological Adaptations of *D. chinense* to Drought–Recovery–Flooding Hydrological Condition

Flooding and submergence pose considerable challenges for plant growth and survival. But, within limits imposed by flooding depth, duration, timing, and intensity, they can, in some species, be overcome by appropriate combinations of growth, morphological, and biochemical and physiological attributes or adaptations [18,20]. In the present study, flooding stimulated many kinds of visible changes in stem portions of flooded seedlings around water levels. In a few days after the initiation of flooding, hypertrophic lenticels began to appear on submerged portions of the stem. One of the normal morphological adaptations of flood-tolerant woody plants is the formation of hypertrophied lenticels, which are the important pathway of gas exchanges between atmosphere and internal tissues in stems and

roots, as well as the oxidation of the rhizosphere [36–38]. Hypertrophied lenticels having abundant intercellular spaces in flooded plants enhance gas diffusion by thermo-osmotic activity [39] and contribute oxygen supply to submerged roots [20,38]. In our experiments, after the drought–recovery treatment, these seedlings were then submitted to flooding (D-R-FF). Numerous adventitious roots began to develop on submerged stems about 20 days after the initiation of flooding. More adventitious roots, as well as hypertrophied lenticels of *D. chinense* at the stem base in the D-R-FF, were observed than those of the FF-R-D. Furthermore, it has been shown that morphological alterations in hydraulic conductivity induced by flooding could exacerbate the susceptibility to drought [40]. Wetland plants use adventitious roots as one of their main adaptation mechanisms to replace existing root systems that have been damaged or whose function has been harmed by stressful circumstances [41–43]. And the rapid development of epicormic shoots in flooding environments would provide a substantial advantage to *D. chinense* species for survival under D-R-FF compared with FF-R-D and FF treatments. Therefore, the early drought stress could facilitate morphological adaptations of *D. chinense* to the later flooding under D-R-FF hydrological condition by more adventitious roots, hypertrophied lenticels, and the stem base compared with the single flooding treatment.

As is generally known in plants, HO degrades free heme released from heme proteins with the generation of ferrous iron (Fe^{2+}), biliverdin IX α (BV-IX α), and carbon monoxide (CO) [44]. CO has been demonstrated to regulate root branching [39,45]. In general, CO in organisms is derived from the degradation of heme whose reaction is strongly acute under drought conditions. And CO induces the formation of more adventitious roots and increases the content of osmoregulatory substances in the plant, enhancing plant adaptation to drought stress [46–48]. Our data showed that more adventitious roots and stem lenticels of drought seedlings occurred significantly compared with fully flooded seedlings. The formation of more adventitious roots and stem hypertrophic lenticels, as well as an increase in stem-base growth of *D. chinense* seedlings, was observed under D-R-FF treatment (Table 3), which occurred coincidentally with enhanced HO activities of *D. chinense* seedlings, with the high CO generation occurring under the adverse environments. It has been shown that the inducible responses of *CsHO1* expression preceded the adventitious root formation [49]. Furthermore, HO induction would be beneficial for adventitious rooting by enhancing the release of CO, a signaling molecular responsible for the adventitious root development [49]. In this present study, it was plausible that more hypertrophied lenticels and adventitious root occurrence may be attributed to the high CO generation due to its regulating a variety of physiological processes under the D-R-FF hydrological regime, which may be an important adaptation of *D. chinense* to alternate drought and flooding stresses.

4.2. Accumulation of Soluble Sugar of *D. chinense* to Drought–Recovery–Flooding Hydrological Condition

Soluble sugar is an important osmoregulatory substance enabling plants to tolerate stress over a long period of time and making a major contribution to cellular osmoregulation [50]. It also acts as a vital signal in the plant developmental regulation and is highly sensitive to environmental stresses [51–53]. However, plant water status is also affected by the accumulation of solutes, e.g., amino acid and soluble sugar, which are involved in the plant metabolism and growth [54]. The accumulation of soluble sugar has long been considered a mechanism for tolerating water stress in some studies [55–58]. For example, a 2-month drought stress experiment triggered a significant increase in the number of soluble sugars in leaves of drought-tolerant *Quercus pubescens* Willd [59]. Similarly, in this study, *D. chinense* seedlings accumulated substantial soluble sugars during D treatment (Figure 10), which would be hydrolyzed and utilized to promote the tolerance of *D. chinense* seedlings to later flooding.

4.3. Enhanced Photosynthesis of *D. chinense* to Drought–Recovery–Flooding Hydrological Condition

The maintenance of relatively high photosynthesis is an important adaptation for flood-tolerant species in aquatic environments. But flood-intolerant species have displayed an appreciable drop in photosynthesis, falling to only 5–25% of unflooded controls [17,60,61]. In this study, the Pn of *D. chinense* seedlings in the D-R-FF was higher than that in the FF (Figure 8). And Pn maintained $1.916 \mu\text{mol m}^{-2} \text{s}^{-1}$ on average value after 28 days of drought. Subsequently, the Pn of *D. chinense* under the D-R-FF treatment was about twice as much as the FF-R-D treatment (Figure 8). It is thus assumed that the maintenance of relatively high Pn is also an important adaptation for *D. chinense* under the D-R-FF hydrological condition.

In the present study, the increase of Pn occurred coincidentally alongside the incremental increase of heme degradation by HO (Figure 9). It is generally known that the role of HO in higher plants is, so far, tightly associated with the pathway leading to phytochrome chromophore metabolism [62,63]. The phytochrome chromophore will increase with increasing BV-IX α derived from the oxidative cleavage of heme by the enzyme HO [64]. The degradation of heme leading to the generation of BV-IX α is a biosynthetic process in photosynthetic organisms [65]. It had been shown that gene expression related to HO was sufficiently active in higher plants to supply for normal photomorphogenesis [64,65]. In this study, higher HO activity exerted a continuous influence on Pn, triggering a positively photomorphogenic response. Pn was higher in the D-R-FF condition than in the FF-R-D due to the higher heme degradation by HO.

Usually, photosynthetic capacity is closely associated with Gs [66,67]. Gs is tightly linked to water vapour pressure difference (VPD) and balances the water supply to seedlings above and below ground. A higher Gs generally occurs when water VPD is lower and the water loss via transpiration is less limited by the substrate's water content under other similar conditions [66]. In this present study, the high Gs in DF may increase gas exchange rates and result in a greater CO₂ inflow. Hence, plants assimilate more photosynthates for growth [68], and then they can rapidly adapt to the later inundation environments. Alterations in Gs would affect leaf water potential by changing Tr [67]. This study confirms a significantly positive relationship between Gs and Tr (Figure 5). Transpiration is the process of water movement through a plant and its evaporation from aerial parts, which determines the amount of water a plant consumes [69]. Additionally, a strong increase in WUE can be caused by a reduction of Gs (rather than an increase of Pn) in response to rising temperature or reduced soil moisture, leading to a stomatal closure as a physiological response to stress [70]. It is typically observed in trees growing in semi-arid regions [71] but also occurs in temperate forests experiencing drying trends [72]. As our data showed, under the NF condition, WUE was also negatively associated with Gs ($r = -0.98, p < 0.01$). The above photosynthetic parameters (Figure 4) and correlation analysis (Figure 5) suggested that *D. chinense* could not only supply adequate water for Gs to enhance Tr in response to DF condition, which is functionally coupled with the enhanced photosynthesis and higher WUE, but also maximize WUE in the NF condition and minimize water loss through transpiration.

According to Farquhar and Sharkey [67], a decline in Pn would be mainly attributed to the stomatal limitation only if both Pn and Ci decline with the increase of Ls. On the contrary, if Ci has a contrary change trend to that of Pn with the decline of Ls, the decline of photosynthesis rate should be attributed to non-stomatal factors, namely, a decline in photosynthetic activity of mesophyll cells, e.g., lower mesophyll carboxylation efficiency, reduced ribulose-1,5-bisphosphate (RuBP) regeneration, or a reduced amount of functional Rubisco, etc. In the present study, Ci follows a different trend of Pn as Ls decreases (DF, Ls = 0.48; NF, Ls = 0.61). This decline in DF on the photosynthesis rate could be attributed to non-stomatal factors. Meanwhile, the formation of more hypertrophied lenticels and adventitious roots and shoot elongation contributed to the gas exchange between internal tissues and the atmosphere, enhancing internal oxygen supply and contributing to photo-

synthetic electron transports, photophosphorylation, and RuBP regeneration [17], which could help restore the reduced photosynthetic rate and stomatal conductance [67].

Chlorophyll content has been shown to be closely linked to a plant's tolerance to stress. Plant chlorophyll concentration varies under stress, triggering early leaf chlorosis, senescence, and abscission [73]. The photosynthetic rate is enhanced with the increase of chlorophyll content only under low-light intensity. Chl a binds more to the photosystem reaction center, while Chl b binds mainly to light-harvesting complexes (LHCs) [74]. Chl b absorbs light energy at wavelengths between 470 and 650 nm, while Chl a cannot effectively absorb light energy in this range. Higher plants use Chl b extensively to absorb light energy over a wider spectrum, which is a crucial component of LHC absorbing, transferring light energy, and maintaining the stability of LHCII to adapt to different situations [75]. The value of Chl a/Chl b was reported to be used as a measurement of the proportion of LHCs and reaction centers (RCs) in thylakoids [76]. In this study, the content of Chl b in the D-R-FF was 18.63% more than that in single FF. And Chl a/Chl b in the D-R-FF was 9.86% less than that in single FF. Similarly, the content of Chl b in the FF-R-D was 20.15% less than that in the D-R-FF (Figure 7B). And Chl a/Chl b in the D-R-FF was 13.56% less than that in the FF-R-D. It could be speculated that Chl b is more stable on LHCs in the D-R-FF hydrological condition, which could assist in sustaining a higher photosynthetic rate.

4.4. Soil Nitrogen and Phosphorus Releasing of *D. chinense* to Drought–Recovery–Flooding Condition

Woodward et al. [77] found long-term enrichment or no changes in soil N contents after repeated drying–wetting cycles. Ye et al. [78] found no changes in soil N contents after repeated drying–wetting cycles, which can affect the forms of N rather than N loss or accumulation. Similarly, our results suggested that repeated drying–wetting cycles had no significant impacts on soil TN of *D. chinense* (Figure 11), which reinforced that TN in the soil may be not sensitive to alternate drought and flooding stresses [79]. Repeated drying–wetting cycles were likely a vital controlling influence for the temporal dynamics of P in the riparian zone [78,80]. In our experiments, the later flooding in the D-R-FF treatment could promote the release of P (D-R-FF > FF > FF-R-D) (Figure 11). And P is also one of the essential nutrients for plant growth and development. Therefore, in the present study, the results showed that soil P was a decisive factor that determined the seedling growth and tolerance of *D. chinense* and was the principal factor in evaluating the endurance capacity of *D. chinense* under alternate drought and flooding stresses. However, it will be further studied how to release soil P and promote P absorption of *D. chinense* under the alternate drought and flooding stresses.

5. Conclusions

This study presented several interesting findings:

- (1) *Distylium chinense* triggered a suite of growth, morphological alterations, and enhanced photo–physiological responses under alternate hydrological conditions and single drought and flooding. The early drought stress could facilitate the tolerance of *Distylium chinense* to the later flooding stress by growth, morphological adaptations, and higher photosynthesis.
- (2) Heme oxygenase degrades free heme released with the generation of carbon monoxide, which may induce the formation of more adventitious roots, enhancing *Distylium chinense* adaptation to early drought stress.
- (3) The increase of net photosynthetic rate due to the increased heme degradation by heme oxygenase in the D-R-FF. And net photosynthetic rate was higher in the D-R-FF than in the FF, followed by alternating FF-R-D and D.
- (4) *Distylium chinense* could supply adequate water for stomatal conductance to enhance transpiration rate in response to drought–flooding conditions, which is functionally coupled with enhanced photosynthesis and higher water-use efficiency.
- (5) Intercellular CO₂ concentration follows a different trend of the net photosynthetic rate as the stomatal limiting value decreases (DF, $L_s = 0.48$; NF, $L_s = 0.61$). This

decline in the alternate drought–flooding condition on the photosynthesis rate could be attributed to non-stomatal factors.

- (6) The soluble sugar accumulation during the prolonged drought period promoted the tolerance of *Distylium chinense* to later flooding. The higher chlorophyll b content to absorb more light energy could assist in maintaining a higher level of photosynthesis in the D-R-FF hydrological condition. Total phosphorus availability via soil has been assumed to be a reaction mechanism to affect the above- and below-ground nutrition supply of *Distylium chinense* seedlings.

These findings will advance our understanding of better adaptations of *Distylium chinense* to alternating D-R-FF treatment compared with alternating FF-R-D and single drought and flooding. Therefore, our results provided basic information about terrestrial wetland plant resilience to managers for the in-situ conservation of *Distylium chinense* and ecological restoration in the hydro-fluctuation zones, wetland ecosystems, and other flood-prone forests where drought–flooding events often occur.

Author Contributions: Conceptualization, methodology, experiments, data curation, software, wrote the original draft, L.Y.; Contributed to additional analyses, experiments, and collected the data, C.Y. and A.A.; Contributed to refining the ideas and collected the data, K.L. and G.H.; Contributed to additional experiments and collected the data, M.H.; Conceptualization, writing—review and editing, funding acquisition, X.L. and Z.Y. All authors have read and agreed to the published version of the manuscript.

Funding: This work was supported by the National Natural Science Foundation of China (No. 51779127), partially funded by Research Project on Seed Preservation Technology and Facilities of Rare Plants in the Three Gorges Reservoir Area—Investigation and Collection of Flooding-Tolerant Germplasm Resources (SDHZ2021346) and Open Project Fund of Key Laboratory of Aquatic Plants and Watershed Ecology, Chinese Academy of Sciences (E0520204). I appreciate having the opportunity to work on this and other relevant projects with everyone.

Data Availability Statement: The original contributions presented in the study are included in the article. The data supporting the conclusions of this article will be made available on request.

Acknowledgments: We are grateful for every reviewer’s valuable comments. We would like to express our gratitude to Youxing Lin for providing constructive information on this study. We also would like to thank Victor Manuel Martinez Espinosa for data collection.

Conflicts of Interest: Author Guiyun Huang and Meixiang Hu were employed by the company China Three Gorges Corporation. The remaining authors declare that the research was conducted in the absence of any commercial or financial relationships that could be construed as a potential conflict of interest.

References

1. Parad, G.A.; Kouchaksaraei, M.T.; Striker, G.G.; Sadati, S.E.; Nourmohammadi, K. Growth, morphology and gas exchange responses of two-year-old *Quercus Castaneifolia* seedlings to flooding stress. *Scand. J. Forest. Res.* **2015**, *31*, 458–466. [[CrossRef](#)]
2. Daniels, A.E.; Cumming, G.S. Conversion or conservation? Understanding wetland change in northwest Costa Rica. *Ecol. Appl.* **2008**, *18*, 49–63. [[CrossRef](#)] [[PubMed](#)]
3. Pucciariello, C.; Perata, P. *Flooding Tolerance in Plants*; CABI Books; CABI International: Oxford, UK, 2012; pp. 148–170. [[CrossRef](#)]
4. Xiang, L.; Li, X.L.; Wang, X.S.; Yang, J.; Lv, K. Genetic diversity and population structure of *Distylium Chinense* revealed by ISSR and SRAP analysis in the Three Gorges Reservoir Region of the Yangtze River, China. *Glob. Ecol. Conserv.* **2020**, *21*, e00805. [[CrossRef](#)]
5. Zhang, Y.Q.; You, Q.L.; Ullah, S.; Chen, C.C.; Shen, L.C.; Liu, Z. Substantial increase in abrupt shifts between drought and flood events in China based on observations and model simulations. *Sci. Total Environ.* **2023**, *876*, 162822. [[CrossRef](#)] [[PubMed](#)]
6. Qiu, J.; Shen, Z.; Leng, G. Synergistic effect of drought and rainfall events of different patterns on watershed systems. *Sci. Rep.* **2021**, *11*, 18957. [[CrossRef](#)] [[PubMed](#)]
7. Ye, C.; Cheng, X.L.; Liu, W.Z.; Zhang, Q.F. Revegetation impacts soil nitrogen dynamics in the water level fluctuation zone of the Three Gorges Reservoir, China. *Sci. Total Environ.* **2015**, *517*, 76–85. [[CrossRef](#)] [[PubMed](#)]
8. Zhang, X.; Dong, Z.C. Impact of the Three Gorges Dam on the hydrology and ecology of the Yangtze River. *Water* **2016**, *8*, 590. [[CrossRef](#)]

9. Li, X.L.; He, D.; Chen, G.; Yang, J. Responses of leaf functional traits to different hydrological regimes and leaf economics spectrum in the water level fluctuation zone of Three Gorges Reservoir, China. *Front. Plant Sci.* **2022**, *13*, 939452. [[CrossRef](#)]
10. Parolin, P.; Lucas, C.; Piedade, M.T.F. Drought responses of flood-tolerant trees in Amazonian floodplains. *Ann. Bot.* **2010**, *105*, 129–139. [[CrossRef](#)]
11. Zhu, Z.H.; Chen, Z.L.; Li, L.; Shao, Y. Response of dominant plant species to periodic flooding in the riparian zone of the Three Gorges Reservoir (TGR), China. *Sci. Total Environ.* **2020**, *747*, 141101. [[CrossRef](#)]
12. Zhang, H.; Zhu, J.; Gong, Z. Abiotic stress responses in plants. *Nat. Rev. Genet.* **2022**, *23*, 104–119. [[CrossRef](#)] [[PubMed](#)]
13. Zaid, A.; Mushtaq, M.; Wani, S.H. Interactions of phytohormones with abiotic stress factors under changing climate. In *Frontiers in Plant-Soil Interaction*, 1st ed.; Tariq, A., Khalid, R.H., Eds.; Academic Press: Cambridge, MA, USA, 2021; pp. 221–236. [[CrossRef](#)]
14. Setter, T.L.; Waters, I. Review of prospects for germplasm improvement for waterlogging tolerance in wheat, barley and oats. *Plant Soil.* **2003**, *253*, 1–34. [[CrossRef](#)]
15. Greenway, H.; Gibbs, J. Review: Mechanisms of anoxia tolerance in plants. II. Energy requirements for maintenance and energy distribution to essential processes. *Funct. Plant Biol.* **2003**, *30*, 999–1036. [[CrossRef](#)]
16. Fukao, T.; Bailey-Serres, J. Plant responses to hypoxia—is survival a balancing act? *Trends Plant Sci.* **2004**, *9*, 449–456. [[CrossRef](#)] [[PubMed](#)]
17. Li, X.L.; Li, N.; Yang, J. Morphological and Photosynthetic Responses of Riparian Plant *Distylium Chinense* Seedlings to Simulated Autumn and Winter Flooding in Three Gorges Reservoir Region of the Yangtze River, China. *Acta Ecol. Sin.* **2011**, *31*, 31–39. [[CrossRef](#)]
18. Li, X.L. Phenotypic Plasticity of Leaves in Relation to Soil Environmental Factors in Heterogeneous Habitats in the Three Gorges Reservoir Region. *Acta Ecol. Sin.* **2018**, *38*, 3581–3591. [[CrossRef](#)]
19. Jackson, M.B.; Ismail, A.M. Introduction to the Special Issue: Electrons, water and rice fields: Plant response and adaptation to flooding and submergence stress. *AoB Plants.* **2015**, *7*, plv078. [[CrossRef](#)]
20. Iwanaga, F.; Yamamoto, F. Effects of flooding depth on growth, morphology and photosynthesis in *Alnus japonica* species. *New For.* **2008**, *35*, 1–14. [[CrossRef](#)]
21. Sun, L.; Li, X.L.; Wang, X.S.; Xiang, L.; Yang, J.; Min, Q.F.; Chen, G.H.; Chen, F.Q.; Huang, C.M.; Wang, G.X. Growth and respiratory metabolic adaptation strategies of riparian plant *Distylium Chinense* to submergence by the field study and controlled experiments. *Plant Physiol. Bioch.* **2020**, *157*, 1–12. [[CrossRef](#)]
22. Jackson, M.B.; Drew, M.C. Effects of flooding on growth and metabolism of herbaceous plants. In *Flooding and Plant Growth*; Kozłowski, E.T., Ed.; Academic Press: Orlando, FL, USA, 1984; pp. 47–128. [[CrossRef](#)]
23. Vasellati, V.; Oesterheld, M.; Medan, D.; Loreti, J. Effects of flooding and drought on the anatomy of *Paspalum dilatatum*. *Ann. Bot.* **2001**, *88*, 355–360. [[CrossRef](#)]
24. Blackman, C.J.; Brodribb, T.J.; Jordan, G.J. Leaf hydraulics and drought stress: Response, recovery and survivorship in four woody temperate plant species. *Plant Cell Environ.* **2009**, *32*, 1584–1595. [[CrossRef](#)]
25. Silva, F.C.E.; Shvaleva, A.; Maroco, J.P.; Almeida, M.H.; Chaves, M.M.; Pereira, J.S. Responses to water stress in two *Eucalyptus globulus* clones differing in drought tolerance. *Tree Physiol.* **2004**, *24*, 1165–1172. [[CrossRef](#)] [[PubMed](#)]
26. Monclus, R.; Villar, M.; Barbaroux, C.; Bastien, C.; Fichot, R.; Delmotte, F.M.; Delay, D.; Petit, J.M.; Brechet, C.; Dreyer, E.; et al. Productivity, water-use efficiency and tolerance to moderate water deficit correlate in 33 poplar genotypes from a *Populus deltoides* × *Populus trichocarpa* F₁ progeny. *Tree Physiol.* **2009**, *29*, 1329–1339. [[CrossRef](#)]
27. Zulfikar, F.; Akram, N.A.; Ashraf, M. Osmoprotection in plants under abiotic stresses: New insights into a classical phenomenon. *Planta* **2020**, *251*, 3. [[CrossRef](#)] [[PubMed](#)]
28. Granda, V.; Delatorre, C.; Cuesta, C. Physiological and biochemical responses to severe drought stress of nine *Eucalyptus globulus* clones: A multivariate approach. *Tree Physiol.* **2014**, *34*, 778–786. [[CrossRef](#)] [[PubMed](#)]
29. Akula, R.; Ravishankar, G.A. Influence of abiotic stress signals on secondary metabolites in plants. *Plant Signal. Behav.* **2011**, *6*, 1720–1731. [[CrossRef](#)] [[PubMed](#)]
30. Zhang, Z.Y.; Chang, H.T.; Endress, P.K. Hamamelidaceae. In *Flora of China*; Wu, Z.Y., Raven, P.H., Hong, D.Y., Eds.; Science Press: Beijing, China, 2003; Volume 9, pp. 18–42.
31. Li, H.S. *Principles and Techniques of Plant Physiological Biochemical Experiment*; Higher Education Press: Beijing, China, 2000.
32. Baslam, M.; Mitsui, T.; Hodges, M.; Priesack, E.; Herritt, M.T.; Aranjuelo, I. Photosynthesis in a Changing Global Climate: Scaling Up and Scaling Down in Crops. *Front. Plant Sci.* **2020**, *11*, 882. [[CrossRef](#)]
33. Hu, M.J.; Guo, Y.P.; Shen, Y.Q.; Zhang, L.C. Environmental Regulation of Citrus Photosynthesis. *Chin. J. Appl. Ecol.* **2006**, *17*, 535–540.
34. Minagawa, J.; Ryutaro, T. Dynamic regulation of photosynthesis in *Chlamydomonas reinhardtii*. *Plant J.* **2015**, *82*, 413–428. [[CrossRef](#)]
35. Schaffer, B.; Whiley, A. Environmental Regulation of Photosynthesis in Avocado Trees—A Mini-Review. In *Proceedings V World Avocado Congress*; Junta de Andalucía: Consejería de Agricultura y Pesca, Spain, 2003; pp. 335–342.
36. Glenz, C.; Schlaepfer, R.; Iorgulescu, I.; Kienast, F. Flooding tolerance of Central European tree and shrub species. *Forest Ecol. and Manag.* **2006**, *235*, 1–13. [[CrossRef](#)]
37. Glenz, C.; Iorgulescu, I.; Kienast, F.; Schlaepfer, R. Modelling the impact of flooding stress on the growth performance of woody species Using Fuzzy Logic. *Ecol. Model.* **2008**, *218*, 18–28. [[CrossRef](#)]

38. Yamamoto, F.; Sakata, T.; Terazawa, K. Physiological, morphological and anatomical response of *Fraxinus mandshurica* Seedlings to Flooding. *Tree Physiol.* **1995**, *15*, 713–719. [[CrossRef](#)] [[PubMed](#)]
39. Buchel, H.B.; Grosse, W. Localization of the porous partition responsible for pressurized gas transport in *Alnus glutinosa* (L.) Gaertn. *Tree Physiol.* **1990**, *6*, 247–256. [[CrossRef](#)] [[PubMed](#)]
40. Hacke, U.G.; Stiller, V.; Sperry, J.S.; Pittermann, J.; McCulloh, K.A. Cavitation fatigue. Embolism and refilling cycles can weaken the cavitation resistance of xylem. *Plant Physiol.* **2001**, *125*, 779–786. [[CrossRef](#)] [[PubMed](#)]
41. Chen, H.J.; Qualls, R.G.; Miller, G.C. Adaptive responses of *Lepidium Latifolium* to soil flooding: Biomass allocation, adventitious rooting, aerenchyma formation and ethylene production. *Environ. Exp. Bot.* **2002**, *48*, 119–128. [[CrossRef](#)]
42. Doležal, J.; Kučerová, A.; Jandová, V.; Klimeš, A.; Říha, P.; Adamec, L.; Schweingruber, F.H. Anatomical adaptations in aquatic and wetland dicot plants: Disentangling the environmental, morphological and evolutionary signals. *Environ. Exp. Bot.* **2021**, *187*, 104495. [[CrossRef](#)]
43. Chen, F.Q.; Xiong, G.M.; Xie, Z.Q. Effects of density on seedling survival and growth of an endangered species *Myricaria Laxiflora*. *Biodivers. Sci.* **2005**, *13*, 332. [[CrossRef](#)]
44. Chen, D.; Brown, J.D.; Kawasaki, Y.; Bommer, J.; Takemoto, J.Y. Scalable production of biliverdin IX α by *Escherichia coli*. *BMC Biotechnol.* **2012**, *12*, 89. [[CrossRef](#)]
45. Guo, K.; Xia, K.; Yang, Z.M. Regulation of tomato lateral root development by carbon monoxide and involvement in auxin and nitric oxide. *J. Exp. Bot.* **2008**, *59*, 3443–3452. [[CrossRef](#)]
46. Zhang, C.; Li, Y.; Yuan, F. Effects of hematin and carbon monoxide on the salinity stress responses of *Cassia obtusifolia* L. seeds and seedlings. *Plant Soil.* **2012**, *359*, 85–105. [[CrossRef](#)]
47. Meng, D.K.; Chen, J.; Yang, Z.M. Enhancement of tolerance of Indian mustard (*Brassica juncea*) to mercury by carbon monoxide. *J. Hazard. Mater.* **2011**, *186*, 1823–1829. [[CrossRef](#)] [[PubMed](#)]
48. Liu, K.; Xu, S.; Xuan, W. Carbon monoxide counteracts the inhibition of seed germination and alleviates oxidative damage caused by salt stress in *Oryza sativa*. *Plant Sci.* **2007**, *172*, 544–555. [[CrossRef](#)]
49. Xuan, W.; Zhu, F.Y.; Xu, S.; Huang, B.K.; Ling, T.F.; Qi, J.Y.; Ye, M.B.; Shen, W.B. The heme oxygenase/carbon monoxide system is involved in the auxin-induced cucumber adventitious rooting process. *Plant Physiol.* **2008**, *148*, 881–893. [[CrossRef](#)] [[PubMed](#)]
50. Du, Y.; Han, Y.; Wang, C.K. The influence of drought on non-structural carbohydrates in the needles and twigs of *Larix gmelinii*. *Acta Ecol. Sin.* **2014**, *34*, 6090–6100.
51. Bartels, D.; Sunkar, R. Drought and Salt Tolerance in Plants. *Crit. Rev. Plant Sci.* **2005**, *24*, 23–58. [[CrossRef](#)]
52. Myers, J.A.; Kitajima, K. Carbohydrate storage enhances seedling shade and stress tolerance in a neotropical forest. *J. Ecol.* **2007**, *95*, 383–395. [[CrossRef](#)]
53. Afzal, S.; Chaudhary, N.; Singh, N.K. Role of soluble sugars in metabolism and sensing under abiotic stress. In *Plant Growth Regulators: Signalling under Stress Conditions*; Aftab, T., Hakeem, K.R., Eds.; Springer: Berlin/Heidelberg, Germany, 2021; pp. 305–334. [[CrossRef](#)]
54. Falchi, R.; Petrusa, E.; Braidot, E.; Sivilotti, P.; Boscutti, F.; Vuerich, M. Analysis of non-structural carbohydrates and xylem anatomy of leaf petioles offers new insights in the drought response of two grapevine cultivars. *Int. J. Mol. Sci.* **2020**, *21*, 1457. [[CrossRef](#)]
55. Wang, Z.; Quebedeaux, B.; Stutte, G. Osmotic adjustment: Effect of water stress on carbohydrates in leaves, stems and roots of apple. *Funct. Plant Biol.* **1995**, *22*, 747. [[CrossRef](#)]
56. Yakushiji, H.; Nonami, H.; Fukuyama, T.; Ono, S.; Takagi, N.; Hashimoto, Y. Sugar accumulation enhanced by osmoregulation in satsuma mandarin fruit. *J. Am. Soc. Horticult. Sci.* **1996**, *121*, 466–472. [[CrossRef](#)]
57. Ogawa, A.; Yamauchi, A. Root osmotic adjustment under osmotic stress in maize seedlings mode of accumulation of several solutes for osmotic adjustment in the root. *Plant Product. Sci.* **2006**, *9*, 39–46. [[CrossRef](#)]
58. Masouleh, S.S.; Aldine, N.J.; Sassine, Y.N. The role of organic solutes in the osmotic adjustment of chilling-stressed plants (vegetable, ornamental and crop plants). *Ornamental Horticult.* **2019**, *25*, 434–442. [[CrossRef](#)]
59. Holland, V.; Koller, S.; Lukas, S.; Brüggemann, W. Drought- and frost- induced accumulation of soluble carbohydrates during accelerated senescence in *Quercus pubescens*. *Trees* **2015**, *30*, 215–226. [[CrossRef](#)]
60. Bradford, K.J. Effect of soil flooding on leaf gas exchange of plants. *Plant Physiol.* **1983**, *73*, 475–479. [[CrossRef](#)] [[PubMed](#)]
61. Chen, H.; Qualls, R.G.; Blank, R.R. Effect of soil flooding on photosynthesis, carbohydrate partitioning and nutrient uptake in the invasive exotic *Lepidium latifolium*. *Aquat. Bot.* **2005**, *82*, 250–268. [[CrossRef](#)]
62. Terry, M.J.; Wahleithner, J.A.; Lagarias, J.C. Biosynthesis of the plant photoreceptor phytochrome. *Arch Biochem. Biophys.* **1993**, *306*, 1–15. [[CrossRef](#)] [[PubMed](#)]
63. Terry, M.J.; Linley, P.J.; Kohchi, T. Making light of it: The role of plant heme oxygenases in phytochrome chromophore synthesis. *Biochem. Soc. Trans.* **2002**, *30*, 604–609. [[CrossRef](#)]
64. Seth, J.D.; Seong, H.B.; Adam, M.D.; Joseph, M.W.; Richard, D.V. The Heme-Oxygenase Family Required for Phytochrome Chromophore Biosynthesis Is Necessary for Proper Photomorphogenesis in Higher Plants. *Plant Physiol.* **2001**, *126*, 656–669. [[CrossRef](#)]
65. Muramoto, T.; Kohchi, T.; Yokota, A.; Hwang, I.; Goodman, H.M. The Arabidopsis photomorphogenic mutant *hy1* is deficient in phytochrome chromophore biosynthesis as a result of a mutation in a plastid heme oxygenase. *The Plant Cell.* **1999**, *11*, 335–348. [[CrossRef](#)]

66. Zhang, A.Y.; Fan, D.Y.; Li, Z.J.; Xiong, G.M.; Xie, Z.Q. Enhanced photosynthetic capacity by perennials in the riparian zone of the Three Gorges Reservoir Area, China. *Ecol. Eng.* **2016**, *90*, 6–11. [[CrossRef](#)]
67. Farquhar, G.D.; Sharkey, T.D. Stomatal Conductance and Photosynthesis. *Annu. Rev. Plant Physiol.* **1982**, *33*, 317–345. [[CrossRef](#)]
68. Souza, A.H.D.; Oliveira, U.S.D.; Oliveira, L.A.; Carvalho, P.H.D.D.; Andrade, M.T.D.; Pereira, T.S.; Junior, C.C.G.; Cardoso, A.A.; Ramalho, J.D.C.; Samuel, C.V.M.; et al. Growth and Leaf Gas Exchange Upregulation by Elevated [CO₂] Is Light Dependent in Coffee Plants. *Plants* **2023**, *12*, 1479. [[CrossRef](#)] [[PubMed](#)]
69. Zhuang, S.D.; Zhou, L.; Xu, W.C.; Xu, N.; Hu, X.Z.; Li, X.Q.; Lv, G.X.; Zheng, Q.H.; Zhu, S.; Wang, Z.L.; et al. Tuning Transpiration by Interfacial Solar Absorber-Leaf Engineering. *Adv. Sci.* **2017**, *5*, 1700497. [[CrossRef](#)]
70. Soumaya, B.; Maxwell, R.S.; Alan, H.T.; Kenneth, J.D.; Rossella, G.; David, J.P.M.; Shelly, A.R. Precipitation alters the CO₂ effect on water-use efficiency of temperate forests. *Glob. Chang. Biol.* **2021**, *27*, 1560–1571. [[CrossRef](#)]
71. Szejner, P.; Wright, W.E.; Belmecheri, S.; Meko, D.; Leavitt, S.W.; Ehleringer, J.R.; Monson, R.K. Disentangling seasonal and interannual legacies from inferred patterns of forest water and carbon cycling using tree-ring stable isotopes. *Glob. Chang. Biol.* **2018**, *24*, 5332–5347. [[CrossRef](#)] [[PubMed](#)]
72. Urrutia-Jalabert, R.; Malhi, Y.; Barichivich, J.; Lara, A.; Delgado-Huertas, A.; Rodríguez, C.G.; Cuq, E. Increased water use efficiency but contrasting tree growth patterns in *Fitzroya cupressoides* forests of southern Chile during recent decades. *J. Geophys.* **2015**, *120*, 2505–2524. [[CrossRef](#)]
73. Casanova, M.T.; Brock, M.A. How do depth, duration and frequency of flooding influence the establishment of wetland plant communities? *Plant Ecol.* **2000**, *147*, 237–250. [[CrossRef](#)]
74. Larcher, W. Physiological plant ecology. 4th edn. *Ann. Bot.* **2004**, *93*, 616–617. [[CrossRef](#)]
75. Yamasato, A.; Nozomi, N.; Ryouichi, T.; Ayumi, T. The N-terminal domain of chlorophyllide a oxygenase confers protein instability in response to chlorophyll b accumulation in Arabidopsis. *Plant Cell.* **2005**, *17*, 1585–1597. [[CrossRef](#)]
76. Panda, D.; Rao, D.N.; Sharma, S.G. Submergence effects on rice genotypes during seedling stage: Probing of submergence driven changes of photosystem 2 by chlorophyll a fluorescence induction O-J-I-P transients. *Photosynthetica* **2006**, *44*, 69–75. [[CrossRef](#)]
77. Woodward, K.B.; Fellows, C.S.; Mitrovic, S.M.; Sheldon, F. Patterns and bioavailability of soil nutrients and carbon across a gradient of inundation frequencies in a lowland river channel, Murray-Darling Basin, Australia. *Agric. Ecosyst. Environ.* **2015**, *205*, 1–8. [[CrossRef](#)]
78. Ye, C.; Chen, C.R.; Butler, O.M.; Rashti, M.R.; Esfandbod, M.; Du, M.; Zhang, Q.F. Spatial and temporal dynamics of nutrients in riparian soils after nine years of operation of the Three Gorges Reservoir, China. *Sci. Total Environ.* **2019**, *664*, 841–850. [[CrossRef](#)] [[PubMed](#)]
79. Han, N.; Hao, Z.; Xu, Y.J. Mechanism of sediment nitrogen release and its contribution to nitrogen output in the alternating flooding and drying conditions of Xiangxi Basin, Jiangxi Province, China. *Environ. Sci.* **2016**, *37*, 534–541. [[CrossRef](#)]
80. Wu, Y.; Wang, X.; Zhou, J.; Bing, H.; Sun, H. The fate of phosphorus in sediments after the full operation of the Three Gorges Reservoir, China. *Environ. Pollut.* **2016**, *214*, 282–289. [[CrossRef](#)] [[PubMed](#)]

Disclaimer/Publisher’s Note: The statements, opinions and data contained in all publications are solely those of the individual author(s) and contributor(s) and not of MDPI and/or the editor(s). MDPI and/or the editor(s) disclaim responsibility for any injury to people or property resulting from any ideas, methods, instructions or products referred to in the content.